Journal of Materials Chemistry C

PAPER

View Article Online
View Journal | View Issue

Cite this: J. Mater. Chem. C, 2015, 3, 734

Investigation of pyrolysis temperature in the one-step synthesis of $L1_0$ FePt nanoparticles from a FePt-containing metallopolymer†

Qingchen Dong,*[ab] Guijun Li,[c] Hua Wang,[a] Philip Wing-Tat Pong,[c] Chi-Wah Leung,*[d] Ian Manners,*[e] Cheuk-Lam Ho,[bg] Hua Li[bf] and Wai-Yeung Wong*[abg]

Received 13th September 2014
Accepted 10th November 2014

DOI: 10.1039/c4tc02058h

www.rsc.org/MaterialsC

Ferromagnetic ($L1_0$ phase) FePt alloy nanoparticles (NPs) with extremely high magnetocrystalline anisotropy are considered to be very promising candidates for the next generation of ultrahigh-density data storage systems. The question of how to generate $L1_0$ FePt NPs with high coercivity, controllable size, and a narrow size distribution is a challenge. We report here a single-step fabrication of $L1_0$ FePt NPs by employing one of the two new polyferroplatinyne bimetallic polymers as precursors. The influence of the pyrolysis temperature on the size and magnetic properties of the resulting FePt alloy NPs has been investigated in detail.

Introduction

Ferromagnetic $L1_0$ phase FePt alloy nanoparticles (NPs) have attracted the growing interest of researchers in the last decade, because of their interesting redox, catalytic and magnetic properties,[1,2] especially their potential application in the next generation of ultrahigh-density magnetic data storage media, which is a consequence of their extraordinarily large uniaxial magnetocrystalline anisotropy $K_u \approx 7 \times 10^6$ J m^{-3} in the bulk phase and high chemical stability.[3–5] FePt NPs are commonly synthesized through refluxing a Fe-source and a Pt-source together in a high boiling organic solvent. However, the superparamagnetic A_1 phase FePt NPs are usually formed first in this way, and a post annealing step is required to give rise to the desirable $L1_0$ phase. Inevitably, some problems such as sintering, agglomeration, broad size distribution, *etc.*, will be concomitant with this method.[6,7] This might be attributed to the fact that the elements Fe and Pt reside in the separate compounds which have different onset decomposition temperatures. Hence, researchers have prepared some organometallic complexes containing both Fe and Pt atoms and subsequently investigated their use as single source precursors to generate the $L1_0$ phase FePt NPs by the one-step decomposition.[8,9] Metallopolymers have attracted intense and increasing research interest over the last two decades[10–14] and are of growing importance in many practical applications, *e.g.* photovoltaic cells,[15] nanocomposites,[16,17] biosensors,[18] polymer light-emitting diodes,[19,20] *etc.* In recent years, researchers have attempted to synthesize metal NPs and metal alloy NPs by utilizing metallopolymers as templates which, on pyrolysis or photolysis, generate NPs with a narrow size distribution and a precisely controllable composition as well as density per unit area.[21–27] In 2008 and 2012, our groups reported a one-pot method to directly synthesize $L1_0$ FePt alloy NPs through the pyrolysis of a metallopolymer containing both Fe and Pt atoms.[28,29] However, no work has been done to investigate the temperature factor of pyrolysis that controls the size and magnetic properties of the resulting alloy NPs. In this work, we report the synthesis of two FePt-containing metallopolymers, followed by one-step generation of $L1_0$ FePt NPs by pyrolyzing the FePt-containing metallopolymers at different temperatures. We also investigated the effect of pyrolysis temperature on the size and magnetic properties of the resulting FePt alloy NPs.

Results and discussion

Synthesis and characterization of target metallopolymers

Synthesis of the target metallopolymers was performed *via* the Sonogashira coupling reaction which gives the macromolecular

[a]MOE Key Laboratory for Interface Science and Engineering in Advanced Materials and Research Center of Advanced Materials Science and Technology, Taiyuan University of Technology, 79 Yingze West Street, Taiyuan 030024, P. R. China. E-mail: dongqingchen@tyut.edu.cn

[b]Institute of Molecular Functional Materials, Department of Chemistry, Partner State Key Laboratory of Environmental and Biological Analysis and Institute of Advanced Materials, Hong Kong Baptist University, Waterloo Road, Kowloon Tong, Hong Kong, P. R. China. E-mail: rwywong@hkbu.edu.hk; Fax: +852-3411-7348

[c]Department of Electrical and Electronic Engineering, The University of Hong Kong, Pokfulam Road, Hong Kong, P. R. China

[d]Department of Applied Physics, Hong Kong Polytechnic University, Hung Hom, Hong Kong, P. R. China

[e]School of Chemistry, University of Bristol, Bristol, BS8 1TS, UK. E-mail: Ian.Manners@bristol.ac.uk

[f]College of Life and Environmental Sciences & Beijing Engineering Research Center of Food Environment and Public Health, Minzu University of China, Beijing 100081, P. R. China

[g]HKBU Institute of Research and Continuing Education, Shenzhen Virtual University Park, Shenzhen 518057, P. R. China

† Electronic supplementary information (ESI) available. See DOI: 10.1039/c4tc02058h

products almost quantitatively. The diethynyl ligands incorporating the ferrocene moiety were prepared first. Then, the coordinated Pt dichloride complex was used to couple with the diethynyl ligands to form the FePt-containing metallopolymers. Scheme 1 shows the chemical structures and the synthetic strategies for the diethynyl ligands **L1** and **L2**. To begin with, commercially available 4-iodotoluene is brominated by *N*-bromosuccinimide (NBS) and benzoyl peroxide in tetrachloromethane to give the corresponding brominated product. Then, the well-known Wittig reaction is involved in preparing the ferrocenylethylene compound. In this practical case, above 90% of the resulting product is in the *trans*-conformation. So, we separate the *trans*-product by column chromatography without further transforming the small amount of the *cis*-compound into a *trans*-one. The *N*-arylation of 3,6-dibromocarbazole and bis(4-bromophenyl)amine was achieved by the modified Ullmann condensation with *p*-iodoarene to result in the production of intermediates **3** and **5**, which then underwent the well-established palladium-catalyzed trimethylsilylethynylation to give trimethylsilyl-terminated compounds **6** and **7**, respectively. Finally, the TMS group was removed in the presence of potassium carbonate in methanol and dichloromethane at room

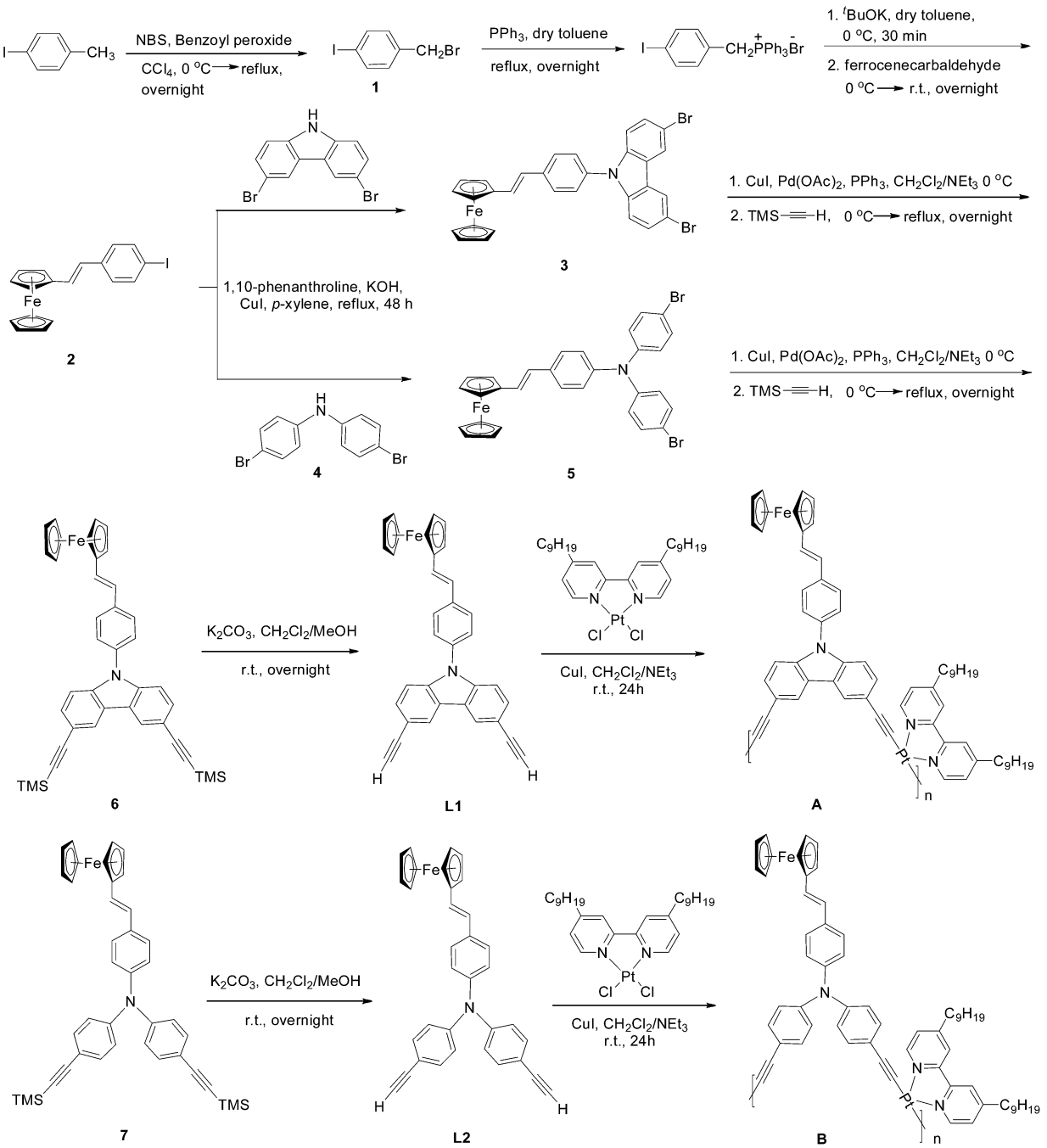

Scheme 1 General synthetic routes to diethynyl ligands **L1** and **L2** as well as their metallopolymers **A** and **B**.

temperature to give diethynyl ligands **L1** and **L2** in up to 95% yields. Metallopolymers **A** and **B** were prepared by the CuI-catalyzed dehydrohalogenation between the Pt(dipyridyl) dichloride precursor and **L1** and **L2**, respectively. Both polymers exhibit low solubility in common organic solvents.

Pyrolysis of FePt-containing metallopolymers

The FePt-containing metallopolymer was placed in a ceramic boat, which was then placed in a tube furnace and subjected to pyrolytic treatment in a nitrogen atmosphere at a heating rate of 20 °C min^{-1} at 600 °C, 700 °C and 800 °C, respectively. Finally, the tube furnace was allowed to cool down to ambient temperature. The NPs synthesized from pyrolysis of metallopolymer **A** at 600 °C, 700 °C and 800 °C were denoted as NP@A-600, NP@A-700 and NP@A-800, respectively, and those from pyrolysis of metallopolymer **B** were denoted as NP@B-600, NP@B-700 and NP@B-800, respectively.

Characterization of the FePt alloy NPs

Powder X-ray diffraction (PXRD) measurement was performed in order to identify the compositions and phases of the resulting NPs as-generated from pyrolysis of metallopolymers **A** and **B** at different temperatures. Fig. 1 shows the PXRD patterns of as-synthesized FePt NPs and Fig. 1(a) is the PXRD pattern of NP@A-600, in which each peak was recognized as an overall reference for other patterns. From this pattern, (001) and (110) peaks (which are the characteristic peaks for $L1_0$ phase FePt alloy NPs[30]) are clearly observed at ~22° and ~33°. All the other samples also show the (001) and (110) peaks as well as apparent splitting of the (200)/(002) peak which signifies the tetragonality of each sample.[9,30] The (111) diffraction peak in each sample appears at $2\theta = 40.96°$, which is consistent with a Fe content of approximately 55 atom%.[30] Besides, no Fe_xN_y and Pt_xN_y phases are observed in these PXRD patterns. Thus, the results of the PXRD measurement suggest that the structure and composition of the resulting NPs correspond to the pure chemically ordered $L1_0$ FePt phase with an atomic ratio of Fe and Pt near unity. Energy-dispersive X-ray (EDX) elemental analysis of the resulting bulk FePt NPs as a powder was also carried out to further verify the composition of each sample. The EDX results are tabulated in Table 1, which manifest that the ratio of Fe and Pt is approximately 50 : 50 as-expected for $L1_0$ phase FePt NPs except for NP@A-800 with a slightly Pt-rich composition. This is in close agreement with the composition as inferred from the (111) peak in the PXRD pattern, and is also consistent with the stoichiometry of the metallopolymer with the near equal atomic ratio of Fe and Pt. Morphologies of the resulting FePt alloy NPs were investigated by transmission electron microscopy (TEM), as shown in Fig. 2. It can be seen clearly that all of the resulting FePt alloy NPs exhibit well-faceted spherical morphology. The insets of Fig. 2 are the high-resolution TEM images of a single FePt NP for each sample, which appeared as uncapped nanocrystals with rounded facets. The continuous fringe-patterns with interplanar distances of around 0.22 nm, corresponding to the (111) *d*-spacing as-expected for $L1_0$ FePt NPs, were observed conspicuously for each sample.[3] The well-faceted shape indicates that the NP is highly crystalline. The NP size distribution of each sample has also been studied by analysis of the corresponding TEM images. Fig. 3 shows the histograms of the size distribution of each sample. As indicated in Fig. 3, the average NP sizes of NP@A-600, NP@A-700 and NP@A-800 are 14.7, 12.9 and 11.3 nm, respectively, with relatively broad size distributions (standard deviation *ca.* 15–21%). While the average NP sizes of NP@B-600, NP@B-700 and NP@B-800 are 7.78, 7.20 and 6.30 nm, respectively, and the size distribution is reasonably narrow (standard deviation *ca.* 9–12%). Hence, NPs generated from metallopolymer **A** render larger size compared to those synthesized from metallopolymer **B**. This could be attributed to the high onset decomposition temperature of metallopolymer **B**, which would result in the relatively fast nucleation of Pt followed by the diffusion of Fe into the Pt nuclei to form

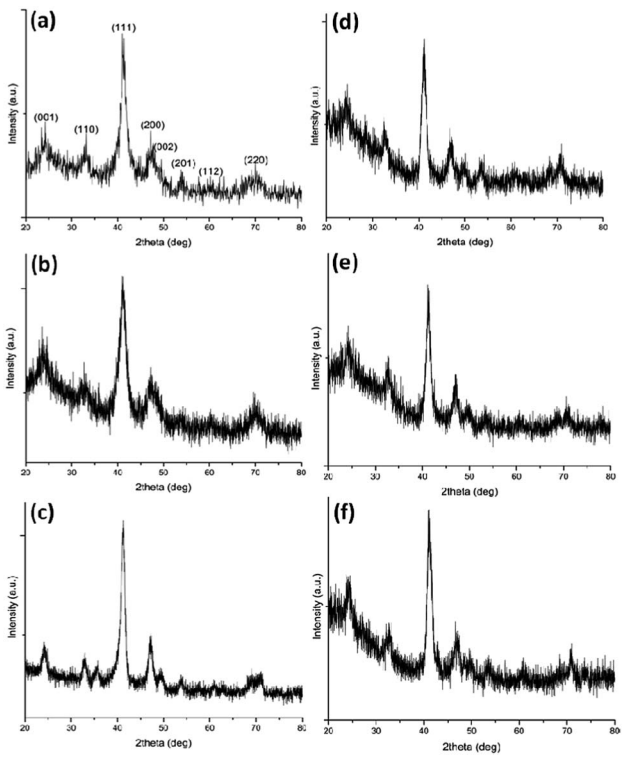

Fig. 1 XRD spectra of as-prepared NPs from pyrolysis of metallopolymers A and B: (a) NP@A-600, (b) NP@A-700, (c) NP@A-800, (d) NP@B-600, (e) NP@B-700 and (f) NP@B-800.

Table 1 EDX results of NPs prepared from polymers A and B

NPs	NP@A-600		NP@A-700		NP@A-800	
	Fe	Pt	Fe	Pt	Fe	Pt
Atomic%	51	49	51	49	54	46
NPs	NP@B-600		NP@B-700		NP@B-800	
	Fe	Pt	Fe	Pt	Fe	Pt
Atomic%	50	50	49	51	49	51

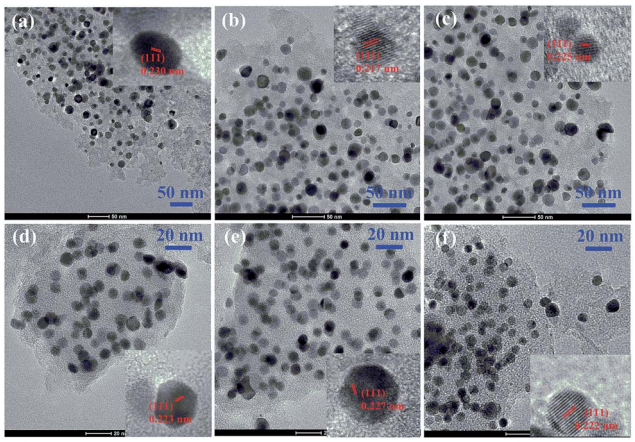

Fig. 2 TEM and high-resolution TEM images of (a) NP@A-600, (b) NP@A-700, (c) NP@A-800, (d) NP@B-600, (e) NP@B-700 and (f) NP@B-800.

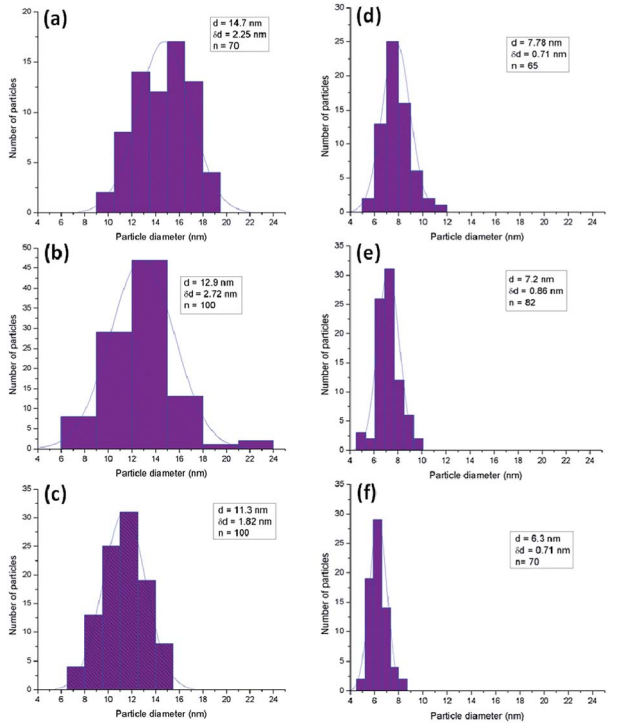

Fig. 3 Particle-size histograms of as-prepared $L1_0$ FePt NPs: (a) NP@A-600, (b) NP@A-700, (c) NP@A-800, (d) NP@B-600, (e) NP@B-700 and (f) NP@B-800.

compact alloy NPs; also, it is noticeable that the average size of the resulting NPs decreases with the increase of the pyrolysis temperature which is quite evident in the case of metallopolymer **B** (Fig. 3). This is because chemical bonds are more rapidly cleaved at higher temperature, and thus more FePt seeds are generated, meanwhile, the organic segments originally bound to the Fe or Pt atoms would protect the FePt seeds from further sintering at higher temperature, which is similar to the function of MgO as reported by Sun *et al.* in 2009.[31]

Magnetic properties of the as-synthesized FePt alloy NPs

Magnetic hysteresis loops recorded for as-prepared bulk FePt NPs as a powder at 300 K are shown in Fig. 4. The coercivity (H_c, an indicator of magnetocrystalline anisotropy) of NP@A-600, NP@A-700 and NP@A-800 is 175.4 Oe, 190.9 Oe, 97.1 Oe, respectively (as indicated in Fig. 4(A)). Therefore, FePt NPs pyrolyzed from metallopolymer **A** at 700 °C hold the highest H_c. While the H_c of NP@B-600, NP@B-700 and NP@B-800 is 312.9 Oe, 209.8 Oe and 622.8 Oe, respectively, demonstrating that 800 °C is the premium temperature for the generation of FePt NPs with the highest H_c using metallopolymer **B** (as indicated in Fig. 4(B)). The relationship of H_c and NP size is plotted in Fig. 5. As we can see, although there is no regular trend of H_c with the shrinkage of NP size, the FePt NPs as-prepared from metallopolymer **B** possess larger H_c in comparison to those from **A** in general. Given the size of the NPs investigated in this work, one would expect that they have single domain behavior, which normally exhibit a rising H_c with increasing particle size;[32] in contrast, the opposite trend was observed in this work. However, it is noted from Fig. 3 that increasing pyrolysis temperature can give rise to smaller NPs. We therefore attribute the observed trend of H_c to the improved crystallinity within

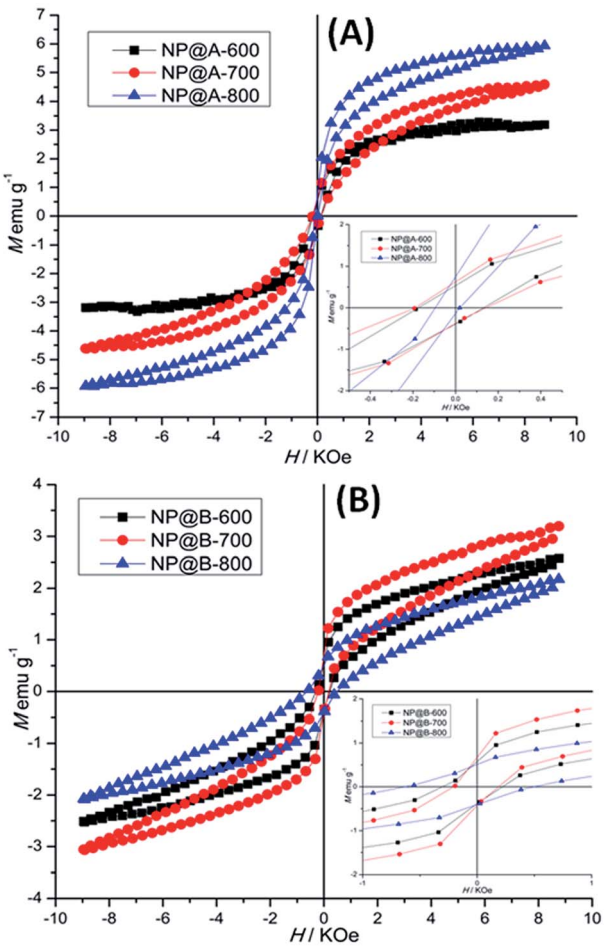

Fig. 4 Hysteresis loops of as-prepared $L1_0$ FePt NPs measured at 300 K. The insets show the enlarged portions.

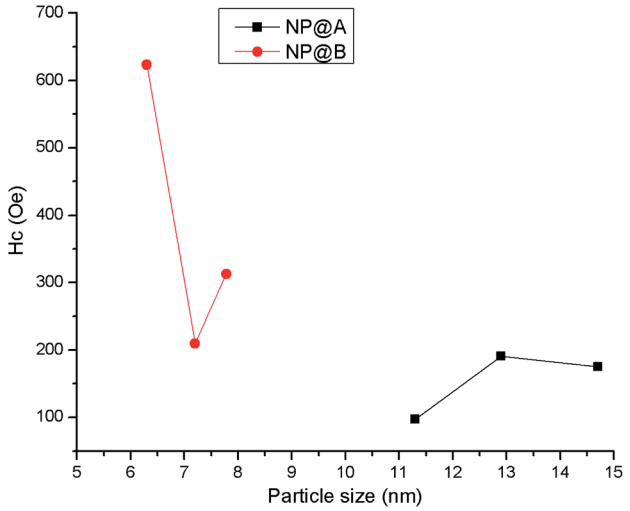

Fig. 5 Relationship between the NP size and coercivity (H_c) of the resulting FePt NPs.

each NP, which is a function of pyrolysis temperature. The presence of grain boundaries within the NP can weaken the exchange coupling within the NP on one hand,[33] and lead to the presence of multiple anisotropy axes (and hence reduced magnetic anisotropy) on the other,[34] both of which cause a reduced H_c.

We also performed magnetic measurements at low temperature for NP@A-700 and NP@B-800 (see Fig. S1 in the ESI†). The results indicate that the H_c of two samples is 680 Oe (NP@A-700) and 1230 Oe (NP@B-800), respectively, which are higher than those at room temperature. More importantly, the low-temperature loops exhibit stronger contributions from the high-coercivity part of the "double coercivity" behavior. These results, together with the absence of secondary phase peaks in the XRD data, suggested that the double coercivity behavior should arise from the existence of a small amount of superparamagnetic $L1_0$ FePt NPs with ultra small size.

Conclusions

We have presented the synthesis of two FePt-containing metallopolymers with an approximately equal atomic ratio of Fe and Pt. By taking the two metallopolymers as precursors, nearly equiatomic $L1_0$ phase FePt NPs were synthesized in a single step without any post annealing treatment as reported previously. Pyrolysis of metallopolymer **A** generated $L1_0$ FePt NPs with an average size of 11.3–14.7 nm while metallopolymer **B** gave rise to $L1_0$ FePt NPs with an average size of 6.3–7.78 nm. Both polymers A and B gave rise to FePt NPs with the smallest average size by pyrolyzing them at 800 °C. The TEM images indicate that the resulting FePt NPs are well-faceted spherical NPs within the carbonaceous matrix which could immobilize and protect the FePt NPs. Magnetic properties of the resulting FePt NPs were investigated by VSM measurements, which manifest that NPs as-synthesized from metallopolymer **B** exhibit higher coercivity as compared to NPs generated from **A** owing to the smaller NP size. Hence, NPs as-prepared at higher temperature have smaller average size and possess larger coercivity. In the future work, we will try to purify these FePt NPs and explore their applications in catalysis or biosensing.

Experimental

General information

All reactions were carried out under nitrogen unless otherwise stated. Commercially available reagents were used as received without further purification. All reactions were monitored by thin-layer chromatography (TLC) with Merck pre-coated glass plates. Compounds were visualized with UV light irradiation at 254 and 365 nm. Separation or purification of products was achieved by column chromatography or preparative TLC using silica gel from Merck (230–400 mesh). NMR spectra were measured in $CDCl_3$ on a Bruker AV 400 NMR instrument with chemical shifts being referenced against tetramethylsilane as the internal standard for ^1H and ^{13}C NMR data. IR spectra were recorded on a Nicolet Magna 550 Series II FTIR spectrometer using KBr pellets for solid state spectroscopy. The positive-ion fast atom bombardment (FAB) mass spectra were recorded in the *m*-nitrobenzyl alcohol matrix on a Finnigan-MAT SSQ710 mass spectrometer. Thermal analyses were performed with a Perkin-Elmer TGA 6 thermal analyzer. The molecular weight of the polymer was determined by GPC using a HP 1050 series HPLC with visible wavelength and fluorescent detectors against polystyrene standards.

Preparation of *p*-bromomethyliodobenzene (1)

To a solution of 4-iodotoluene (1.414 g, 6.48 mmol) in 15 mL of tetrachloromethane were added, with stirring and in an ice-water bath, *N*-bromosuccinimide (1.153 g, 6.48 mmol) and benzoyl peroxide (40 mg). The mixture was warmed at reflux temperature overnight. Afterwards, the mixture was filtered and the solvent was removed to give a residual solid which was purified by chromatography on a silica gel column using *n*-hexane/dichloromethane (5 : 1, v/v) as an eluent. *p*-Bromomethyliodobenzene was isolated as a white solid: 1.635 g (85%). ^1H NMR ($CDCl_3$, 400 MHz, δ/ppm): 7.68 (d, $J = 8.0$ Hz, 2H, Ar-H), 7.14 (d, $J = 8.0$ Hz, 2H, Ar-H), 4.42 (s, 2H, ArCH_2); FAB-MS: m/z 413.90 (M^+).

Preparation of 1-ferrocenyl-2-(*p*-iodophenyl)-ethene (2)

A solution of triphenylphosphine (177 mg, 0.67 mmol) in 20 mL of anhydrous toluene and *p*-bromomethyliodobenzene (200 mg, 0.67 mmol) was warmed at reflux temperature overnight to give a white solid that was filtered and washed with toluene. *p*-Iodobenzyltriphenylphosphonium bromide is a white solid: 356 mg (95%). In a three-necked round-bottom flask, previously flamed and under an argon atmosphere, in an ice-water bath, was placed *p*-iodobenzyltriphenylphosphonium bromide (250 mg, 0.45 mmol) dispersed in anhydrous toluene (15 mL). To this mixture was added potassium *tert*-butoxide (76 mg, 0.675 mmol) and, after 30 min, the solution took an intense orange colour. Into this was dropped a solution of

ferrocenecarbaldehyde (96 mg, 0.45 mmol) in dry toluene (5 mL). After 30 min, the mixture was stirred at room temperature overnight. Then, the solvent was removed and the residual solid was extracted with dichloromethane and purified by silica gel column chromatography using *n*-hexane/dichloromethane (8 : 1, v/v) as an eluent. 1-Ferrocenyl-2-(*p*-iodophenyl)-ethene was obtained as an orange solid: (298.1 mg, 72%). ^{1}H NMR ($CDCl_3$, 400 MHz, δ/ppm): 7.63 (d, $J = 8.0$ Hz, 2H, Ar-*H*), 7.17 (d, $J = 8.0$ Hz, 2H, Ar-*H*), 6.88 (d, $J = 16$ Hz, 1H, C*H*=CH), 6.60 (d, $J = 16$ Hz, 1H, CH=C*H*), 4.46, 4.45 (s, 2H, Fc-*H*), 4.30, 4.30 (s, 2H, Fc-*H*), 4.14 (s, 5H, Fc-*H*); ^{13}C NMR ($CDCl_3$, 125 MHz, δ/ppm): 137.64, 137.39, 128.02, 127.49, (Ar), 124.71, 91.50 (C=C), 77.21, 69.41, 69.23, 66.94 (Fc).

Preparation of *N*-(*p*-2-ferrocenyl-ethenyl-phenyl)-3,6-dibromocarbazole (3)

To a solution of 1-ferrocenyl-2-(*p*-iodophenyl)-ethene (318 mg, 0.77 mmol) and 3,6-dibromocarbazole (200 g, 0.615 mmol) in 8 mL *p*-xylene, 1,10-phenanthroline (16.5 mg, 0.092 mmol) and potassium hydroxide (120 mg, 2.15 mmol) were added respectively. After the mixture was stirred at 80–100 °C for 30 min, copper iodide (17.5 mg, 0.092 mmol) and potassium hydroxide (120 mg, 2.15 mmol) were added, and the solution was allowed to reflux at 140 °C for 3 days. Then, the mixture was extracted with chloroform, and the combined organic layer was washed with water, and dried over Na_2SO_4. The solvent was removed and purified by silica gel column chromatography using *n*-hexane/dichloromethane (5 : 1, v/v) as an eluent. *N*-(*p*-2-ferrocenyl-ethenyl-phenyl)-3,6-dibromocarbazole was obtained as an orange solid (385 mg, 63%). ^{1}H NMR ($CDCl_3$, 400 MHz, δ/ppm): 8.20 (s, 2H, Ar-*H*), 7.65 (d, $J = 8.0$ Hz, 2H, Ar-*H*), 7.51 (d, $J = 8.0$ Hz, 2H, Ar-*H*), 7.44 (d, $J = 8.0$ Hz, 2H, Ar-*H*), 7.28 (d, $J = 8.0$ Hz, 2H, Ar-*H*), 6.99 (d, $J = 16$ Hz, 1H, C*H*=CH), 6.78 (d, $J = 16$ Hz, 1H, CH=C*H*), 4.52 (s, 2H, Fc-*H*), 4.34 (s, 2H, Fc-*H*), 4.18 (s, 5H, Fc-*H*); ^{13}C NMR ($CDCl_3$, 125 MHz, δ/ppm): 139.82, 137.81, 134.88, 129.36, 128.64, 127.14, 127.09, 124.54, 123.90, 123.19 (Ar), 113.01, 111.57 (C=C), 82.75, 69.36, 69.29, 67.05 (Fc); FAB-MS: m/z 611.00 (M^+).

Preparation of bis(4-bromophenyl)amine (4)

To a stirred solution of diphenylamine (8.46 g, 50 mmol) in 50 mL of DMF at 0 °C was added dropwise a solution of *N*-bromosuccinimide (17.8 g, 100 mmol) in 50 mL DMF over 30 min. The resulting solution was allowed to stir at 0 °C for a further 6 h. Then, water was added under vigorous stirring to afford the dibrominated compound as a pure white product which was filtered off and dried *in vacuo* (16.26 g, 99%). ^{1}H NMR ($CDCl_3$, 400 MHz, δ/ppm): 7.36 (d, $J = 8.0$ Hz, 4H, Ar-*H*), 6.92 (d, $J = 8.0$ Hz, 4H, Ar-*H*), 5.65 (s, 1H, N*H*); ^{13}C NMR ($CDCl_3$, 125 MHz, δ/ppm): 141.69, 132.30, 119.48, 113.37 (Ar-*C*).

Preparation of *N*-(*p*-2-ferrocenyl-ethenyl-phenyl)-3,8-dibromobiphenylamine (5)

The procedure for the preparation of **5** was similar to that of **3**. The resulting product was obtained as a brown-yellow solid (426 mg, 57%). ^{1}H NMR ($CDCl_3$, 400 MHz, δ/ppm): 7.36–7.31 (m, 6H, Ar-*H*), 6.99–6.94 (m, 6H, Ar-*H*), 6.79 (d, $J = 16$ Hz, 1H, C*H*=CH), 6.64 (d, $J = 16$ Hz, 1H, CH=C*H*), 4.45 (s, 2H, Fc-*H*), 4.28 (s, 2H, Fc-*H*), 4.14 (s, 5H, Fc-*H*); ^{13}C NMR ($CDCl_3$, 125 MHz, δ/ppm): 146.34, 145.43, 133.48, 132.36, 126.82, 126.14, 125.16 (Ar), 124.61, 115.49 (C=C), 83.45, 69.22, 69.03, 66.77 (Fc).

Preparation of *N*-(*p*-2-ferrocenyl-ethenyl-phenyl)-3,6-bis(trimethylsilylethynyl)carbazole (6)

To an ice-cooled mixture of **3** (372 mg, 0.609 mmol) in a freshly distilled triethylamine (10 mL) and CH_2Cl_2 (10 mL) solution mixture were added CuI (20 mg), $Pd(OAc)_2$ (20 mg) and PPh_3 (20 mg). After the solution was stirred for 30 min at 0 °C, trimethylsilylacetylene (0.52 mL, 3.7 mmol) was then added and the suspension was stirred for 30 min in an ice-bath before being warmed to room temperature. After reacting for 30 min at room temperature, the mixture was heated to 70–80 °C for 24 h. The solution was then allowed to cool to room temperature and the solvent mixture was evaporated *in vacuo*. The crude product was purified by column chromatography on silica gel with a solvent combination of CH_2Cl_2/ethyl acetate (5 : 1, v/v) as an eluent to provide *N*-(*p*-2-ferrocenyl-ethenyl-phenyl)-3,6-bis(trimethylsilyl-ethynyl)carbazole as an orange-yellow solid (240 mg, 61%). ^{1}H NMR ($CDCl_3$, 400 MHz, δ/ppm): 8.24, (d, $J = 8.0$ Hz, 2H, Ar-*H*), 7.63 (d, $J = 8.0$ Hz, 2H, Ar-*H*), 7.52 (d, $J = 8.0$ Hz, 2H, Ar-*H*), 7.45 (d, $J = 8.0$ Hz, 2H, Ar-*H*), 7.31 (d, $J = 8.0$ Hz, 2H, Ar-*H*), 6.98 (d, $J = 16$ Hz, 1H, C*H*=CH), 6.78 (d, $J = 16$ Hz, 1H, CH=C*H*), 4.52 (s, 2H, Fc-*H*), 4.33 (s, 2H, Fc-*H*), 4.17 (s, 5H, Fc-*H*), 0.29 (s, 18H, $SiMe_3$); ^{13}C NMR ($CDCl_3$, 125 MHz, δ/ppm): 140.75, 137.57, 134.77, 130.11, 128.37, 126.97, 126.93, 124.44, 122.60, 114.68 (Ar), 109.79, 105.97 (C=C), 92.25, 82.65 (C≡C), 77.08, 69.36, 69.29, 67.05 (Fc); FAB-MS: m/z 645.40 (M^+).

Preparation of *N*-(*p*-2-ferrocenyl-ethenyl-phenyl)-3,6-bis(trimethylsilyl-ethynyl)biphenylamine (7)

The procedure for the preparation of **7** was similar to that of **6**. The resulting product was obtained as an orange-yellow solid (253 mg, 63%) ^{1}H NMR ($CDCl_3$, 400 MHz, δ/ppm): 7.37–7.34 (m, 6H, Ar-*H*), 7.04–6.99 (m, 6H, Ar-*H*), 6.82 (d, $J = 16$ Hz, 1H, C*H*=CH), 6.67 (d, $J = 16$ Hz, 1H, CH=C*H*), 4.47 (s, 2H, Fc-*H*), 4.30 (s, 2H, Fc-*H*), 4.16 (s, 5H, Fc-*H*), 0.26 (s, 18H, $SiMe_3$); ^{13}C NMR ($CDCl_3$, 125 MHz, δ/ppm): 147.12, 145.06, 133.78, 133.02, 126.74, 126.23, 125.26, 125.13 (Ar), 123.18, 116.99 (C=C), 105.03, 93.58 (C≡C), 83.39, 69.16, 68.97, 66.73 (Fc); FAB-MS: m/z 647.40 (M^+).

Preparation of *N*-(*p*-2-ferrocenyl-ethenyl-phenyl)-3,6-diethynylcarbazole (L1)

A mixture of **6** (230 mg, 0.356 mmol) and K_2CO_3 (111 mg, 0.803 mmol) in a mixture of methanol (8 mL) and CH_2Cl_2 (8 mL) was stirred overnight under a nitrogen atmosphere at room temperature. The completion of the reaction was verified by spot TLC. The solvent was removed by rotary evaporation. The resulting mixture was redissolved in CH_2Cl_2 (40 mL) and washed with three portions of 20 mL water. The light yellow organic phase was dried over anhydrous sodium sulfate and evaporated to dryness. The crude product was

purified by column chromatography on silica gel eluting with hexane to provide **L1** as an orange solid (171 mg, 96%). ^{1}H NMR ($CDCl_3$, 400 MHz, δ/ppm): 8.27 (d, J = 0.8 Hz, 2H, Ar-*H*), 7.65 (d, J = 8.0 Hz, 2H, Ar-*H*), 7.57 (d, J = 1.6 Hz, 2H, Ar-*H*), 7.55 (d, J = 1.6 Hz, 2H, Ar-*H*), 7.46 (d, J = 8.4 Hz, 2H, Ar-*H*), 7.00 (d, J = 16 Hz, 1H, C*H*═CH), 6.78 (d, J = 16 Hz, 1H, CH═C*H*), 4.52 (s, 2H, Fc-*H*), 4.34 (s, 2H, Fc-*H*), 4.18 (s, 5H, Fc-*H*), 3.10 (s, 2H, C≡C–*H*); ^{13}C NMR ($CDCl_3$, 125 MHz, δ/ppm): 141.11, 137.84, 134.81, 130.45, 128.64, 127.17, 124.73, 124.60, 122.71 (Ar), 113.81, 110.16 (C═C), 84.59, 82.80 (C≡C), 75.89, 69.41, 69.35, 67.10 (Fc); FAB-MS: m/z 502.20 (M^+); IR (KBr): 2104 ($\upsilon_{C\equiv C}$) cm^{-1}, 3295 ($\upsilon_{C\equiv C-H}$) cm^{-1}.

Preparation of *N*-(*p*-2-ferrocenyl-ethenyl-phenyl)-4,4-diethynyl-biphenylamine (L2)

The procedure for the preparation of **L2** was similar to that of **L1**. The resulting product was obtained as an orange-red solid (145 mg, 98%) ^{1}H NMR ($CDCl_3$, 400 MHz, δ/ppm): 7.36 (m, 6H, Ar-*H*), 7.03–7.01 (m, 6H, Ar-*H*), 6.81 (d, J = 16 Hz, 1H, C*H*═CH), 6.65 (d, J = 16 Hz, 1H, CH═C*H*), 4.45 (s, 2H, Fc-*H*), 4.28 (s, 2H, Fc-*H*), 4.14 (s, 5H, Fc-*H*), 3.05 (s, 2H, C≡C–*H*); ^{13}C NMR ($CDCl_3$, 125 MHz, δ/ppm): 147.41, 145.01, 134.03, 133.21, 126.84, 126.41, 125.54, 125.10 (Ar), 123.20, 115.94 (C═C), 83.62, 83.36 (C≡C), 77.15, 69.20, 69.03, 66.78 (Fc); FAB-MS: m/z 503.20 (M^+); IR (KBr): 2102 ($\upsilon_{C\equiv C}$) cm^{-1}, 3283 ($\upsilon_{C\equiv C-H}$) cm^{-1}.

Preparation of [$PtCl_2$(^{n}Non_2bipy)]

A suspension of K_2PtCl_4 (100 mg, 0.245 mmol) in water was mixed with 4,4′-dinonyl-2,2′-bipyridyl (^{n}Non_2bipy, 101.6 mg, 0.245 mmol). Then, a drop of concentrated HCl was added as a catalyst. The reaction mixture was allowed to warm at 60 °C and stirred overnight. The reaction mixture was then cooled down to room temperature and extracted with dichloromethane. The crude product was purified by column chromatography on silica gel eluting with dichloromethane to provide [$PtCl_2$(^{n}Non_2bipy)] as a bright yellow solid (140 mg, 85%). ^{1}H NMR ($CDCl_3$, 400 MHz, δ/ppm): 9.17 (s, 2H, Ar-*H*), 7.89 (s, 2H, Ar-*H*), 7.20, 7.18 (d, J = 6.0 Hz, 2H, Ar-*H*), 2.81 (t, J = 8.0 Hz, 4H, CH_2CH$_2$), 1.76–1.72 (m, 4H, CH$_2$CH_3), 1.41–1.28 (m, 24H, CH$_2$CH_2CH$_2$), 0.88 (t, J = 1.6 Hz, 6H, CH$_2$CH_3); ^{13}C NMR ($CDCl_3$, 125 MHz, δ/ppm): 156.60, 156.39, 148.18, 126.41, 123.81 (Ar), 35.86, 32.28, 30.03, 29.95, 29.72, 27.23, 25.32, 23.05, 14.12 (C_9H_{19}).

Synthesis and characterization of the metallopolymers

Since the metallopolymers **A** and **B** were prepared by a similar procedure, the typical method for the copper(I)-catalyzed dehydrohalogenation reaction is illustrated here by the preparation of metallopolymer **A**. To a solution of **L1** (30 mg, 0.12 mmol) in 30 mL of CH_2Cl_2/triethylamine (1 : 1, v/v) were added [$PtCl_2$(^{n}Non_2bipy)] (81 mg, 0.12 mmol) and CuI (5 mg). The mixture was allowed to stir at room temperature for 24 h under a nitrogen atmosphere. Afterwards, the solvent was removed and the residue was redissolved in a small amount of CH_2Cl_2 and reprecipitated from methanol. Centrifugation was performed to give **A** as a red solid (yield: 93%). Metallopolymer **B** was isolated as a red solid with a yield of 90%. For **A**: IR (KBr): 2107 ($\upsilon_{C\equiv C}$) cm^{-1}; GPC (THF): M_w = 90 390, M_n = 52 080, M_w/M_n = 1.74; anal. calcd for $C_{62}H_{65}N_3FePt$: C, 67.51; H, 5.94; N, 3.81. Found: C, 67.32; H, 6.10; N, 3.98%; T_{decomp} (°C): 356 °C. For **B**: IR (KBr): 2104 ($\upsilon_{C\equiv C}$) cm^{-1}; GPC (THF): M_w = 115 230, M_n = 98 390, M_w/M_n = 1.17; anal. calcd for $C_{62}H_{67}N_3FePt$: C, 67.38; H, 6.11; N, 3.80. Found: C, 67.55; H, 6.43; N, 4.08%; T_{decomp} (°C): 321 °C.

Pyrolysis of metallopolymers

The as-synthesized metallopolymer was placed in a ceramic boat, which was then placed inside a quartz reaction tube equipped with temperature and gas-flow controls. Then, the whole set-up was heated to the desired temperature at a rate of 20 °C min^{-1} under a nitrogen atmosphere.

Nanoparticle characterization

Structural characterization of as-synthesized FePt NPs was performed by PXRD on a Bruker AXS D8 Advance X-ray Diffractometer machine, with $CuK_{\alpha 1}$ (λ = 540 nm, 40 kV, dan 40 mA) for analyzing the composition and phase purity of the resulting NPs. TEM was performed using a Tecnai G2 20 S-TWIN for probing the morphology, particle size and size distribution of NPs. EDX spectra were obtained using a LEO 1530 scanning electron microscope for studying the ratio of Fe and Pt in the resulting metal alloy NPs. Magnetic properties of the as-prepared FePt NPs were investigated at room temperature and 100 K by using a Lakeshore 7407 vibrating sample magnetometer (VSM), with an applied field up to 2 T.

Acknowledgements

We acknowledge the financial support from the National Natural Science Foundation of China (Grant no.: 61307030, 61205179, 21101111, and 51373145), Hong Kong Research Grants Council (HKBU203312), Hong Kong Baptist University (FRG2/12-13/083), Areas of Excellence Scheme, University Grants Committee of HKSAR (AoE/P-03/08) and Hundred Talents Program of Shanxi Province. The work was also supported by the Partner State Key Laboratory of Environmental and Biological Analysis (SKLP-14-15-P011) and Strategic Development Fund of HKBU. Q. Dong acknowledges the financial support from the Program for the Outstanding Innovative Teams of Higher Learning Institutions of Shanxi (OIT), Fund Program for the Scientific Activities of Selected Returned Overseas Professionals in Shanxi Province, the Natural Science Foundation for Young Scientists of Shanxi Province, China (Grant no.: 2014021019-2), the Outstanding Young Scholars Cultivating Program, Research Project Supported by Shanxi Scholarship Council of China (Grant no.: 2014–02) and the Qualified Personal Foundation of Taiyuan University of Technology (Grant no.: 2013Y003, tyut-rc201275a). CWL acknowledges financial support from PolyU (A-PM21/G-YL07). H. Li thanks the 111 Project and Beijing Engineering Research Center of Food Environment and Public Health from the Minzu University of China (no. B08044 and no. 10301-01404026) for

financial support. We also thank Dr Q. Wang for assistance with the polymer synthesis.

Notes and references

1 S. Sun, *Adv. Mater.*, 2006, **18**, 393–403.
2 N. A. Frey, S. Peng, K. Cheng and S. Sun, *Chem. Soc. Rev.*, 2009, **38**, 2532–2542.
3 S. Sun, C. B. Murray, D. Weller, L. Folks and A. Moser, *Science*, 2000, **27**, 1989–1992.
4 (*a*) D. Weller and A. Moser, *IEEE Trans. Magn.*, 1999, **35**, 4423–4439; (*b*) J. P. Wang, *Proc. IEEE*, 2008, **96**, 1847–1863.
5 A. Moser, *J. Phys. D: Appl. Phys.*, 2002, **35**, R157–R167.
6 T. Thomson, S. L. Lee, M. F. Toney, C. D. Dewhurst, F. Y. Ogrin, C. J. Oates and S. Sun, *Phys. Rev. B: Condens. Matter Mater. Phys.*, 2005, **72**, 064441–064447.
7 H. L. Nguyen, L. E. Howard, G. W. Stinton, S. R. Giblin, B. K. Tanner, I. Terry, A. K. Hughes, I. M. Ross, A. Serres and J. S. O. Evans, *Chem. Mater.*, 2006, **18**, 6414–6418.
8 A. Capobianchi, M. Colapietro, D. Fiorani, S. Foglia, P. Imperatori, S. Laureti and E. Palange, *Chem. Mater.*, 2009, **21**, 2007–2009.
9 M. S. Wellons, W. H. Morris, Z. Gai, J. Shen, J. Bentley, J. E. Wittig and C. M. Lukehart, *Chem. Mater.*, 2007, **19**, 2483–2488.
10 V. Bellas and M. Rehahn, *Angew. Chem., Int. Ed.*, 2007, **46**, 5082–5104.
11 G. R. Whittell, M. D. Hager, U. S. Schubert and I. Manners, *Nat. Mater.*, 2011, **10**, 176–188.
12 K. A. Williams, A. J. Boydston and C. W. Bielawski, *Chem. Soc. Rev.*, 2007, **36**, 729–744.
13 B. J. Holliday and T. M. Swager, *Chem. Commun.*, 2005, 23–36.
14 W. Y. Wong and C. L. Ho, *Coord. Chem. Rev.*, 2006, **250**, 2627–2690.
15 W. Y. Wong, X. Z. Wang, Z. He, A. B. Djurišić, C. T. Yip, K. Y. Cheung, H. Wang, C. S. K. Mak and W. K. Chan, *Nat. Mater.*, 2007, **6**, 521–527.
16 M. L. Mejía, K. Agapiou, X. Yang and B. J. Holliday, *J. Am. Chem. Soc.*, 2009, **131**, 18196–18197.
17 M. L. Mejía, G. Reeske and B. J. Holliday, *Chem. Commun.*, 2010, **46**, 5355–5357.
18 P. Bertoncello and R. J. Forster, *Biosens. Bioelectron.*, 2009, **24**, 3191–3200.
19 W.-Y. Wong, *Dalton Trans.*, 2007, 4495–4510.
20 M. A. Rawashdeh-Omary, J. M. López-de-Luzuriaga, M. D. Rashdan, O. Elbjeirami, M. Monge, M. Rodriguez-Castillo and A. Laguna, *J. Am. Chem. Soc.*, 2009, **131**, 3824–3825.
21 J. B. Gilroy, S. K. Patra, J. M. Mitchels, M. A. Winnik and I. Manners, *Angew. Chem., Int. Ed.*, 2011, **50**, 5851–5855.
22 K. Liu, S. B. Clendenning, L. Friebe, W. Y. Chan, X. Zhu, M. R. Freeman, G. C. Yang, C. M. Yip, D. Grozea, Z. H. Lu and I. Manners, *Chem. Mater.*, 2006, **18**, 2591–2601.
23 S. B. Clendenning, S. Aouba, M. S. Rayat, D. Grozea, J. B. Sorge, Z. H. Lu, C. M. Yip, M. R. Freeman, H. E. Ruda and I. Manners, *Adv. Mater.*, 2004, **16**, 215–219.
24 S. B. Clendenning, S. Han, N. Coombs, C. Paquet, M. S. Rayat, D. Grozea, P. M. Brodersen, R. N. S. Sodhi, C. M. Yip, Z. H. Lu and I. Manners, *Adv. Mater.*, 2004, **16**, 291–296.
25 J. B. Shi, C. J. W. Jim, F. Mahtab, J. Z. Liu, J. W. Y. Lam, H. H. Y. Sung, I. D. Williams, Y. P. Dong and B. Z. Tang, *Macromolecules*, 2010, **43**, 680–690.
26 J. Liu, J. W. Y. Lam, M. Häussler, A. Qin and B. Z. Tang, *J. Inorg. Organomet. Polym. Mater.*, 2009, **19**, 133–138.
27 W. Z. Yuan, J. Z. Sun, J. Z. Liu, Y. Dong, Z. Li, H. P. Xu, A. Qin, M. Häussler, J. K. Jin, Q. Zheng and B. Z. Tang, *J. Phys. Chem. B*, 2008, **112**, 8896–8905.
28 K. Liu, C. L. Ho, S. Aouba, Y. Q. Zhao, Z. H. Lu, S. Petrov, N. Coombs, P. Dube, H. E. Ruda, W. Y. Wong and I. Manners, *Angew. Chem., Int. Ed.*, 2008, **47**, 1255–1259.
29 Q. C. Dong, G. J. Li, C. L. Ho, M. Faisal, C. W. Leung, P. W. T. Pong, K. Liu, B. Z. Tang, I. Manners and W. Y. Wong, *Adv. Mater.*, 2012, **24**, 1034–1040.
30 T. J. Klemmer, N. Shukla, C. Liu, X. W. Wu, E. B. Svedberg, O. Mryasov, R. W. Chantrell, D. Weller, M. Tanase and D. E. Laughlin, *Appl. Phys. Lett.*, 2002, **81**, 2220–2222.
31 J. Kim, C. Rong, J. P. Liu and S. Sun, *Adv. Mater.*, 2009, **21**, 906–909.
32 C. B. Rong, D. Li, V. Nandwana, N. Poudyal, Y. Ding and Z. L. Wang, *Adv. Mater.*, 2006, **18**, 2984–2988.
33 G. Herzer, *IEEE Trans. Magn.*, 1989, **25**, 3327–3329.
34 W. Scholz, J. Fidler, T. Schrefl, D. Suess, H. Forster, R. Dittrich and V. Tsiantos, *J. Magn. Magn. Mater.*, 2004, **272–276**, 1524–1525.